Pressure-Induced Change from Activation to Diffusion Control in Fast Reactions of Carbon Monoxide with Hemes

Teddy G. Traylor,*,† Jikun Luo,† Jerald A. Simon,‡ and Peter C. Ford*,‡

Contribution from the Department of Chemistry-0506, University of California at San Diego, 9300 Gilman Drive, La Jolla, California 92093-0506, and Department of Chemistry, University of California at Santa Barbara, Santa Barbara, California 93106. *Received November 1, 1991*

Abstract: Increasing hydrostatic pressure from 1 to 3000 atm in toluene solutions of chelated protoheme–carbon monoxide resulted in an increase in the bimolecular rate of carbon monoxide after photolysis of the complex. When the same series of kinetic measurements were made in the more viscous solvent mineral oil, the bimolecular combination rate increased with pressure up to about 1000 atm and decreased over the range of 2000–3000 atm. These results indicate a change of rate limiting step from bond formation to diffusion as the pressure is increased. This provides confirmation of conclusions based upon picosecond kinetic studies, clarifies some of the mysteries concerning carbon monoxide binding to heme proteins, and points up the fact that the carbon monoxide binding mechanism differs significantly from those of all other simple ligands. Carbon monoxide reacts with five-coordinated heme compounds with activation control at low viscosity. Other ligands such as isocyanides and imidazoles react with diffusion controlled rates. These findings are discussed in the context of heme protein reactions with ligands.

Introduction

Geminate chemical processes in solution have recently gained renewed interest due to the development of ultrafast laser photolysis techniques[1,2] and the occurrence of such processes in biological oxygen transport systems.[3-15] There are several recent studies of picosecond kinetics of biomimetic model systems which have the same imidazole–protoheme–ligand system (BHmL) found in the active sites of many proteins.[6,7,16,17] Each of the BHmL systems photolyzed led to efficient labilization of L, and at ordinary solvent viscosities all returned partially to the bound state in less than 40 ps except when L = carbon monoxide.[6,7,17,18] Even in the more viscous solvent mineral oil, carbon monoxide return could not be observed in the time period of 1–8000 ps.[17] Similar results were obtained with myoglobin, confirming earlier studies of hemeproteins.[5] By greatly increasing the viscosity of the system by using glycerol as solvent, geminate return of carbon monoxide was observed.[8,17,19-21] The values of the rate constants obtained have been interpreted in terms of a bond-making rate constant of about 10^9 s^{-1}.[17] The results for all ligands studied were interpreted in terms of a single contact pair intermediate having different rates of collapse to the bound state for different ligands. Only one concentration independent process was observed in each reaction at low solvent viscosity.[8,17]

$$\mathrm{BHmL} \underset{k_{-1}}{\overset{h\nu,\ k_1}{\rightleftharpoons}} [\mathrm{BHm\ L}] \underset{k_{-2}}{\overset{k_2}{\rightleftharpoons}} \mathrm{BHm} + \mathrm{L} \qquad (1)$$

From the overall rate constants, the quantum yields upon picosecond photolysis, and the concentration-independent rates, values of k_2 and k_{-2} were calculated to be 3.8×10^{10} s^{-1} and 3×10^8 M^{-1} s^{-1}, respectively, for MeNC at low viscosity. The k_{-1} values for MeNC and CO were proposed to differ, the calculated values being $\sim 8 \times 10^{10}$ s^{-1} for MeNC and 10^9 s^{-1} for CO.[17]

According to this interpretation the rates of binding of isocyanides to BHm are diffusion controlled, proceeding at least 50% to the bound state for each formation of the intermediate. By contrast, only a small fraction of the intermediate for L = CO leads to the bound state, thus this reaction is activation controlled. A positive activation volume for isocyanide binding, corresponding to $\Delta V^{\ddagger}$ for viscous flow in a diffusion-controlled reaction ($k_{-1} > k_2$), was observed.[22] In contrast, the binding of carbon monoxide was found to have a negative activation volume, consistent with rate-limiting bond formation ($k_{-1} < k_2$). Therefore, the principal difference between carbon monoxide and other ligands in normal solvents is that all ligands except carbon monoxide react with BHm with diffusion control.

* To whom correspondence and reprint requests should be addressed.
† University of California at San Diego.
‡ University of California at Santa Barbara.

(1) Ippen, E. P.; Shank, C. V. *Appl. Phys. Lett.* **1975**, *27*, 488-490.
(2) Ippen, E. P.; Bergman, A. *Chem. Phys. Lett.* **1976**, *38*, 611-614.
(3) Shank, C. V.; Ippen, E. P.; Bersohn, R. *Science* **1976**, *193*, 50-51.
(4) Nõe, L. J.; Eisert, W. G.; Rentzepis, P. M. *Proc. Natl. Acad. Sci., U.S.A.* **1978**, *75*, 573-577.
(5) (a) Greene, B. I.; Hochstrasser, R. M.; Weisman, R. B.; Eaton, W. A. *Proc. Natl. Acad. Sci., U.S.A.* **1978**, *75*, 5255-5259. (b) Postlewaite, J. C.; Miers, J. B.; Dlott, D. D. *J. Am. Chem. Soc.* **1989**, *111*, 1248-1255. (c) Frauenfelder, H.; Nienhaus, G. U.; Johnson, J. B. *J. Phys. Chem.* **1991**, *95*, 272-278.
(6) Jongeward, K. A.; Magde, D.; Taube, D. J.; Marsters, J. C.; Traylor, T. G.; Sharma, V. S. *J. Am. Chem. Soc.* **1988**, *110*, 380-387.
(7) Traylor, T. G.; Magde, D.; Taube, D. J.; Jongeward, K. A. *J. Am. Chem. Soc.* **1987**, *109*, 5864-5865.
(8) Marden, M. C.; Hazard, E. S., III; Gibson, Q. H. *Biochemistry* **1986**, *25*, 2786-2792.
(9) (a) Moore, J. N.; Hansen, P. A.; Hochstrasser, R. M. *Chem. Phys. Lett.* **1987**, *138*, 110-116. (b) Anfinrud, P. A.; Han, C.; Hochstrasser, R. M. *Proc. Natl. Acad. Sci., U.S.A.* **1989**, *86*, 8387-8391.
(10) Momenteau, M.; Loock, B.; Tetreau, C.; Lavallette, D.; Croisy, A.; Shaeffer, C.; Huel, C.; Lhoste, J.-M. *J. Chem. Soc., Perkin Trans 2* **1987**, 249-257.
(11) Rohlfs, R. J.; Olson, J. S.; Gibson, Q. H. *J. Biol. Chem.* **1988**, *263*, 1803-1813.
(12) Tetreau, C.; Lavallette, D.; Momenteau, M.; Lhoste, J. M. *Proc. Natl. Acad. Sci., U.S.A.* **1987**, *84*, 2267-2271.
(13) Doster, W.; Bowne, S. F.; Frauenfelder, H.; Reinisch, L.; Shyamsunder, E. *J. Mol. Biol.* **1987**, *194*, 299-312.
(14) Traylor, T. G.; Berzinis, A. P. *Proc. Natl. Acad. Sci., U.S.A.* **1980**, *77*, 3171-3175.
(15) (a) Traylor, T. G.; Taube, D. J.; Jongeward, K. A.; Magde, D. *J. Am. Chem. Soc.* **1990**, *112*, 6875-6880. (b) Jongeward, K. A.; Magde, D.; Taube, D. J.; Traylor, T. G. *J. Biol. Chem.* **1988**, *263*, 6027-6030.
(16) Berinstain, A. B.; English, A. M.; Hill, B. C. *J. Am. Chem. Soc.* **1990**, *112*, 9649-9651.
(17) (a) Traylor, T. G.; Magde, D.; Taube, D. J.; Jongeward, K. A.; Bandyopadhyay, D.; Luo, J.; Walda, K. N. *J. Am. Chem. Soc* **1992**, *114*, 417-429. (b) Taube, D. J.; Traylor, T. G.; Magde, D.; Walda, K.; Luo, J. Submitted for publication. (c) Traylor, T. G.; Magde, D.; Luo, J.; Walda, K. N.; Bandyopadhyay, D.; Wu, G. In press. (d) Traylor, T. G.; Luo, J.; Magde, D.; Walda, K. N. In preparation.
(18) Henry, E. R.; Sommer, J. H.; Hofrichter, J.; Eaton, W. A. *J. Mol. Biol.* **1983**, *166*, 443.
(19) (a) Moore, J. N.; Hansen, P. A.; Hochstrasser, R. M. *Chem. Phys. Lett.* **1987**, *138*, 110-116. (b) Anfinrud, P. A.; Han, C.; Hochstrasser, R. M. *Proc. Natl. Acad. Sci., U.S.A.* **1989**, *86*, 8387-8391.
(20) (a) Petrich, J. W.; Poyart, C.; Martin, J. L. *Biochemistry* **1988**, *27*, 4049-4060. (b) Martin, J. L.; Migus, A.; Poyart, C.; Lecarpentier, Y.; Astier, R.; Antonette, A. *Proc. Natl. Acad. Sci., U.S.A.* **1983**, *80*, 173-177. (c) Lingle, R., Jr.; Xu, X.; Zhu, H.; Yu, S.; Hopkins, J. B.; Straub, K. D. *J. Am. Chem. Soc.* **1991**, *113*, 3992.
(21) (a) Petrich, J. W.; Poyart, C.; Martin, J. L. *Biochemistry* **1988**, *27*, 4049-4060. (b) Martin, J. L.; Migus, A.; Poyart, C.; Lecarpentier, Y.; Astier, R.; Antonette, A. *Proc. Natl. Acad. Sci., U.S.A.* **1983**, *80*, 173-177. (c) Lingle, R., Jr.; Xu, X.; Zhu, H.; Yu, S.; Hopkins, J. B.; Straub, K. D. *J. Am. Chem. Soc.* **1991**, *113*, 3992.

0002-7863/92/1514-4340$03.00/0

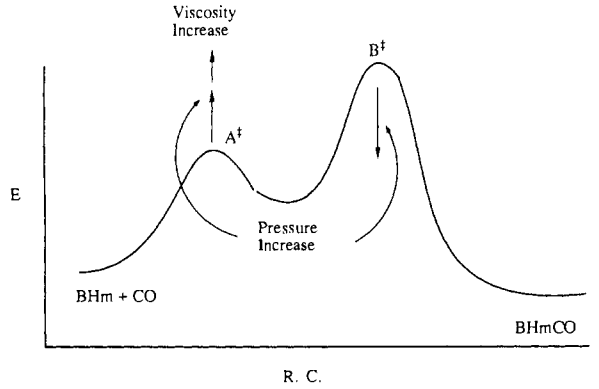

Figure 1. Illustration of expected effects of pressure and solvent viscosity on the mechanistic steps depicted in eq 1.

The fact that very high viscosity brings about geminate rebinding of carbon monoxide and the observation that the bimolecular rate constant, the reaction of BHm with carbon monoxide, is 10^7 M^{-1} s^{-1}, only 20 to 30 times slower than the diffusion-controlled bimolecular reactions with isocyanides, imidazoles, ethers, nitric oxide, etc., suggested that reaction with carbon monoxide is near diffusion controlled. The observation of Caldin and Hasinoff[23] that $\Delta V^{\ddagger}$ for carbon monoxide binding to protoheme in glycerol is positive seems to suggest diffusion control in this viscous solvent. Because this system involves a heme without proximal imidazole and a highly polar solvent, we cannot compare the results with those of the pressure study of a five-coordinated BHmCO complex in a nonpolar solvent.

It appears that most reactions of iron(II) prophyrins with ligands are diffusion controlled in low or high viscosity solvents whereas the reaction with carbon monoxide is activation controlled in low viscosity solvents and diffusion controlled at very high viscosities.

It has been suggested that most bimolecular reactions would change to diffusion control at sufficiently high viscosity or pressure.[24-27] It should therefore be possible to choose a range of viscosities and pressures where this change could be observed directly as a change in the sign of $\Delta V^{\ddagger}$. This idea is illustrated in Figure 1.

Because solvent viscosity and pressure-induced viscosity both affect diffusion but only pressure is expected to affect bond formation within the geminate pair (Figure 1) a judicious choice of solvent viscosity might allow the activation free energy $A^{\ddagger}$ to be raised above $B^{\ddagger}$ within a convenient range of pressures. Therefore, we have studied the effect of pressure on the rate of reaction of chelated protoheme with carbon monoxide in hydrocarbon solvents of different viscosities and have confirmed the prediction that, at the right viscosity, a change in the rate-limiting step can be induced by an increase in hydrostatic pressure. These observations also confirm the kinetics of the cage processes in this reaction which were determined by picosecond spectroscopy and relate the photoprocesses to the thermal processes.

Experimental Section

Materials. Toluene was distilled over calcium hydride. Light mineral oil (Whiteworth), sodium dithionite (Aldrich), and 18-crown-6 (Aldrich) were used without further purification. Carbon monoxide from Matheson was used as purchased. Chelated protoheme chloride ($MCPH^+Cl^-$) was from previous studies.[7] Toluene was deoxygenated by bubbling carbon monoxide through the solvent for 2 h.

Sample Preparations. (a) Monochelated Protoheme–CO (MCPH–CO) in Toluene. Protohemin 3-(1-imidazolyl)propylamide stearyl ester chloride ($MCPH^+Cl^-$)[7] was dissolved in a minimum amount of CH_2Cl_2 and added to toluene (3 mL). After carbon monoxide bubbling for 2 h, the hemin solution was reduced by adding a saturated solution of sodium dithionite/18-crown-6/methanol (3 μL). The reduced solution was diluted with carbon monoxide-saturated toluene (3–4 mL) so that the Soret absorbance was about 1.5 in a 5-mm quartz cuvette. The UV–vis spectrum was taken before each experiment.

(b) MCPH–CO in Mineral Oil. Concentrated MCPH–CO toluene solution was produced by the above procedure. Mineral oil was degassed by heating to near the boiling point under high vacuum, pumped overnight, and then saturated with carbon monoxide. The MCPH–CO toluene solution was added to mineral oil (3 mL) until the Soret absorbance was 1.5 in a 5-mm quartz cuvette. The final compositions of the solvents were 95/5, 90/10, 85/15 (v/v) mineral oil/toluene. The UV–vis spectrum was taken before the experiment.

The sample (~0.8 mL) was loaded under carbon monoxide atmosphere into a cylindrical quartz capsule (25 mm in length, 5 mm in diameter) that was subsequently capped with a Teflon piston with two Viton O-rings (the capsule/piston combination was designed to transmit the applied pressure without exchanging solution with the surrounding medium). The capsule was placed into a high-pressure spectroscopic cell. The high-pressure cell was then filled with pressure-transmitting fluid (water) and sealed.

Instrumentation. The photophysical measurements were performed at the University of California, Santa Barbara on an instrument described in detail elsewhere.[28] Simply, the pseudo-first-order rates of carbon monoxide rebinding to the ferrous five-coordinated heme in a pressure cell were measured with a Quanta Ray DCR-1A Nd/YAG pulse laser (30 mJ per pulse, with a duration of 10 ns based on the carbon monoxide recombination measurement) with the harmonic generator operating at both 532 and 355 nm as the excitation source (10 Hz). A Corning 7.37 band-pass filter was used to ensure spectral purity of the exciting light, and a quartz lens was used to focus the laser beam down to the size of the high-pressure cell windows. The kinetics were monitored by watching the disappearance of the five-coordinated heme at 435 nm, and the output signal was displayed as absorption intensity versus time on a Tektronix 7904 oscilloscope. The high-pressure cell was a modified Nova-Swiss Model 545.0040 (four sapphire optical windows; maximum working pressure 400 MPa). The pressure was generated by an Enerpac hand pump, measured at the primary stage with a Heise 47053 pressure gauge, and transmitted to the high-pressure cell by means of a pressure multiplier. The sample was contained in a capsule. The pressure transmitting fluid was water.

Experimental Procedure for Rate Measurements. All experiments were carried out at room temperature (23 ± 1 °C). A period of 10–20 min was allowed for temperature equilibration subsequent to changing pressure in the cell. Lifetime measurements were generally made over the following approximate pressure sequence in order to check for any hysteresis (there was none in the reported data): ambient pressure, 1500 atm, 3000 atm, 500 atm, 2500 atm, 2000 atm, 1000 atm, and ambient pressure. Thirty-two laser shots were collected for each run. The lifetime of the reaction was obtained from the first-order curve fitting of the original curve. The final data came from the average of 4 runs of 32 shots each.

Results

The effect of pressure on the reaction of chelated protoheme (MCPH)[7] with carbon monoxide in mineral oil/toluene solutions was investigated to determine whether the appropriate combination of solvent viscosity and hydrostatic pressure can induce a change in the rate-limiting step of a bimolecular reaction. In each case the chelated protoheme in the appropriate solvent was equilibrated with CO (P_{CO} = 1 atm) at ambient hydrostatic pressure, and the sample was placed in a sealed quartz capsule with no gas phase CO in contact with the liquid sample. Consequently, the only changes in [CO] (estimated to be 0.0075 M at ambient pressure) would be the result of solvent compressibility over the range of applied pressure.[29]

(22) Taube, D. J.; Projahn, H.; van Eldik, R.; Magde, D.; Traylor, T. G. *J. Am. Chem. Soc.* **1990**, *112*, 6880–6886.
(23) Caldin, E. F.; Hasinoff, B. B. *J. Chem. Soc., Faraday Trans. 1* **1975**, *71*, 515–521.
(24) Hamann, S. D. *Faraday Soc. Trans.* **1958**, *54*, 507.
(25) Nicholson, A. E.; Norrish, R. G. W. *Faraday Soc. Discuss.* **1956**, *22*, 104.
(26) van Eldik, R.; Asano, T.; le Noble, W. *J. Chem. Rev.* **1989**, *89*, 549.
(27) Asano, T.; le Noble, W. *J. Chem. Rev.* **1978**, *78*, 407.
(28) (a) Weber, W.; DiBenedetto, J.; Offen, H.; van Eldik, R.; Ford, P. C. *Inorg. Chem.* **1984**, *23*, 2033–2038. (b) DiBenedetto, J.; Arkle, V.; Goodwin, H.; Ford, P. C. *Inorg. Chem.* **1985**, *24*, 455–456. (c) Crane, D. R.; Ford, P. C. *J. Am. Chem. Soc.* **1990**, *112*, 6871–6875.
(29) Although the compressibility of the present mixed solvent systems is unknown, the pressure dependence of [CO] can be estimated from Bridgman's data for the compressibility of *n*-decane (Bridgman, P. W. *The Physics of High Pressure*; Harvard University Press: Cambridge, 1958; 129). From these data, one can estimate that the pressure-induced changes in [CO] due to solvent compressibility make a contribution of ca. −1 cm^3 mol^{-1} to the apparent volumes of activation reported here.

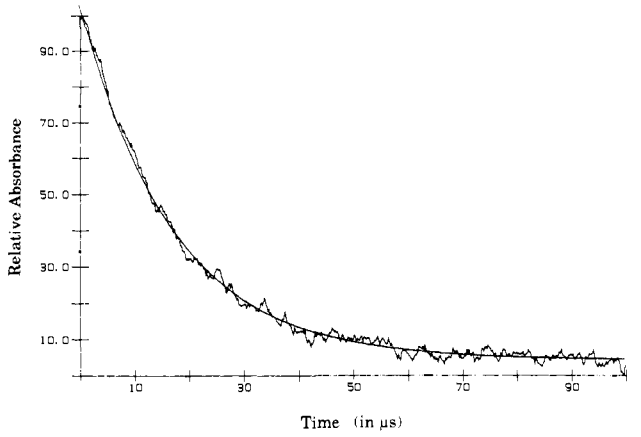

Figure 2. Representative decay curve and exponential curve fitting for the absorbance changes at 430 nm resulting from reaction of CO with monochelated protoheme subsequent to nanosecond photoexcitation of the carbonyl complex at 355 nm. Solution conditions: solvent is 95/5 (v/v) mineral oil/toluene, [heme] = 1.0×10^{-5} M, [CO] = 7.8×10^{-3} M, hydrostatic pressure is 1000 atm, T = 25 °C. The first-order rate constant k_{obs} obtained by the curve fitting is 5.9×10^4 s^{-1}.

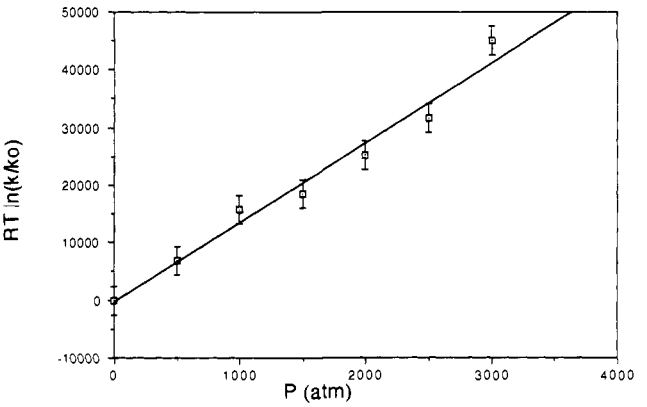

Figure 3. Plot of RT ln ($k_{obs}/k°$) vs hydrostatic pressure for the reaction of CO with the intermediate BHm formed by ns laser flash photolysis of BHm–CO in neat toluene solution: [heme] = 1.0×10^{-5} M, [CO] = 7.5×10^{-3} M, T = 25 °C. The apparent activation volume is the negative of the slope, in this case the value being $\Delta V^{\ddagger}_{app} = -13.7 \pm 1.4$ cm^3 mol^{-1}.

The decay of the transient absorbance changes following nanosecond flash photolysis of these solutions was exponential in each case investigated as illustrated by the representative data of Figure 2. In neat toluene the rate increases with increasing pressure throughout the range 1–3000 atm, and a plot of RT ln ($k_{obs}/k°$) vs P is linear (Figure 3, $k°$ is the rate constant measured at ambient pressure). From the slope of this plot can be calculated[30] the apparent activation volume $\Delta V^{\ddagger}_{app} = -13.7 \pm 1.4$ cm^3 mol^{-1}, a value somewhat less negative than that obtained previously with a different instrument.[22] The negative value of this $\Delta V^{\ddagger}$ indicates that, under these conditions, the reaction is activation controlled, i.e., k_{-1} is rate limiting.

Figure 4 demonstrates that the effect of pressure on the reaction rates in solutions which are largely mineral oil is entirely different. In this case, k_{obs} increases with pressure to ~1000 atm and then decreases as pressure is raised further. The data illustrated in Figure 4 (a plot of RT ln ($k_{obs}/k°$) vs P for rates measured in 90/10 (v/v) mineral oil/toluene) indicate two regimes where linear relationships are apparent. In the low-pressure regime (<1000 atm), the resulting $\Delta V^{\ddagger}_{app}$ was calculated to have a value of −9.6 cm^3 mol^{-1} while in the higher pressure regime the $\Delta V^{\ddagger}_{app}$ displayed

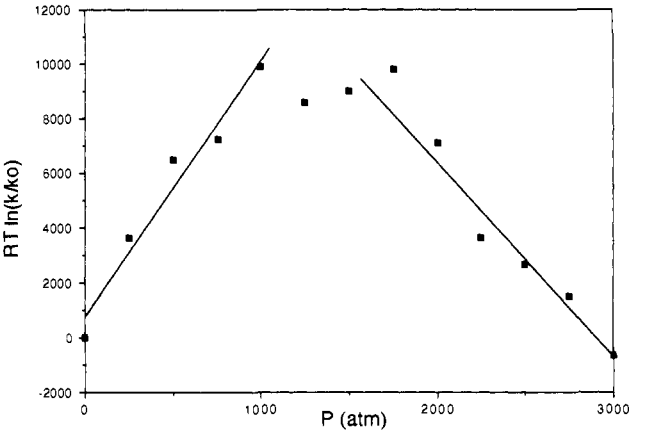

Figure 4. Plot of RT ln ($k_{obs}/k°$) vs hydrostatic pressure for the reaction of CO with the intermediate BHm formed by nanosecond laser flash photolysis of BHm–CO in 90/10 (v/v) mineral oil/toluene solution: [heme] = 1×10^{-5} M, [CO] = 7.5×10^{-3} M, T = 25 °C. The lines drawn are from linear least-squares analysis of the data recorded for the pressure range 0–1000 atm ($\Delta V^{\ddagger}_{app} = -9.6$ cm^3 mol^{-1}) and for the range 2000–3000 atm ($\Delta V^{\ddagger}_{app} = +7.1$ cm^3 mol^{-1}) for this single run.

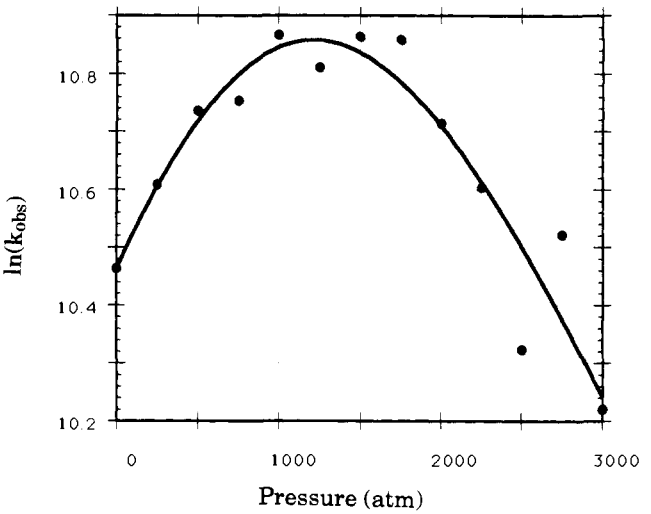

Figure 5. Plot of RT ln (k_{obs}) vs hydrostatic pressure for the collected data of six runs investigating the pressure effect on the reaction of CO with the intermediate BHm formed by nanosecond laser flash photolysis of BHm–CO in mineral oil/toluene solution 90/10 to 95/5 (v/v): [heme] = 1×10^{-5} M, [CO] = 7.5×10^{-3} M, T = 25 °C. The curve shown is a mathematical fit to these data based on the model described by eq 1 (see ref 32).

a positive value of +7.1 cm^3 mol^{-1}. A number of similar experiments were carried out for solutions ranging from 90/10 to 95/5 (v/v) mineral oil/toluene, and in each case an analogous bimodal relationship was noted with a negative $\Delta V^{\ddagger}_{app}$ in the low-pressure regime and a positive $\Delta V^{\ddagger}_{app}$ in the high-pressure regime. From run to run, there was considerable scatter in the $\Delta V^{\ddagger}_{app}$ values calculated by using the assumption of linearity in the respective regimes. This scatter can be attributed in part to the difficulty in obtaining rate data for a large number of different pressures with a single sample owing to the slow degradation of the substrate under the high light intensities used.[31] Nonetheless, if the relative rate data for all the runs are plotted on a single figure, the curve seen in Figure 5 is the result, clearly indicating that, despite some variations in the solvent composition, the bimodal behavior is extremely consistent. Linear regression analysis gives a negative $\Delta V^{\ddagger}_{app}$ of ca. −10 cm^3 mol^{-1} over the pressure range 1–1000 atm and a positive $\Delta V^{\ddagger}_{app}$ of ca. +11 cm^3 mol^{-1} over the pressure range

(30) (a) The volume of activation for any dynamic excited state process is defined by $\Delta V^{\ddagger}_i = -RT(\mathrm{d} \ln k_i/\mathrm{d}P)_T$; therefore the slope of the plot in Figure 3 is $\Delta V^{\ddagger}_i/RT$. (b) Ford, P. C. In *Inorganic High Pressure Chemistry, Kinetics and Mechanisms*; van Eldik, R., Ed.; Elsevier: Amsterdam, 1986; Chapter 6, pp 295–338.

(31) In the cylindrical cell of the high-pressure apparatus, transient absorbance changes tend to be relatively small and give larger experimental uncertainties at the higher pressure where Φ_d values are smaller (see text).

2000–3000 atm. The curve shown in Figure 5 is a numerical fit to these data based on the model described by eq 1.[32,33]

This unprecedented behavior is qualitatively consistent with the model described above. The observed rates in toluene and in the mineral oil/toluene mixtures are virtually the same at ambient pressure, and both systems display negative $\Delta V^{\ddagger}_{app}$ values at lower pressures. Only in the more viscous mineral oil/toluene mixtures do the rates show the positive $\Delta V^{\ddagger}_{app}$ values seen at higher pressure.

Earlier studies determined the quantum yield for CO photodissociation (Φ_d) from BHm–CO to be ~1.0 as was also observed for myoglobin–CO.[34] In the present experiments, this value was assumed for the ambient pressure experiments, and relative quantum yields were determined at various hydrostatic pressures by comparing the absorbance changes recorded immediately after flash photolysis. In each experiment only a small fraction of substrate was photolyzed, so the relative ΔAbs values are directly proportional to the relative Φ_d values. In neat toluene solution, there was a modest drop in Φ_d with pressure. A value of 0.81 ± 0.9 mol/einstein was determined at 3000 atm. In mineral oil/toluene (94/6 (v/v)), Φ_d proved to be much more pressure sensitive with values of 0.65 ± 0.05 and 0.40 ± 0.07 being recorded at 1500 and 3000 atm, respectively.

Discussion

The qualitative interpretation of these changes in $\Delta V^{\ddagger}$ with pressure is straightforward when considered in terms of the three-state model which has been established for iron(II) porphyrin reactions with ligands (eq 1).

In diffusion controlled reactions, such as those with isocyanides, k_{-2} is rate limiting and $\Delta V^{\ddagger}$ is positive.[22] In contrast, for the activation controlled reaction of carbon monoxide in toluene, k_{-1} is rate limiting and $\Delta V^{\ddagger}$ is negative.[22] Formation of BHmCO from the solvent-separated species will have the rate form

$$\frac{d[BHm–CO]}{dt} = k_{obs}[BHm][CO] \quad (2)$$

where

$$k_{obs} = \frac{k_{-1}k_{-2}[CO]}{k_{-1} + k_2} = (\tau)^{-1} \quad (3)$$

The apparent volumes of activation are defined by

$$\Delta V^{\ddagger}_{obs} = -RT\left(\frac{d \ln k_{obs}}{dP}\right)_T \quad (4)$$

If it is assumed that [CO] is constant throughout a pressure run,

$$\Delta V^{\ddagger}_{obs} = -RT\left\{\left(\frac{d \ln k_{-2}}{dP}\right)_T + \left(\frac{d \ln k_{-1}}{dP}\right)_T - \left(\frac{d \ln (k_{-1} + k_2)}{dP}\right)_T\right\} = \Delta V^{\ddagger}_{-2} + \Delta V^{\ddagger}_{-1} + RT\left(\frac{d \ln (k_{-1} + k_2)}{dP}\right)_T \quad (5)$$

Consider two limiting cases, the first being that the reaction is activation limited, the second being that the reaction is diffusion limited. An example of the first limiting case would be the reaction as observed in pure toluene solution. In this limit $k_2 \gg k_{-1}$ and eq 5 would then be

$$\Delta V^{\ddagger}_{obs} = \Delta V^{\ddagger}_{-2} + \Delta V^{\ddagger}_{-1} + RT\left(\frac{d \ln (k_{-1} + k_2)}{dP}\right)_T = \Delta V^{\ddagger}_{-2} + \Delta V^{\ddagger}_{-1} - \Delta V^{\ddagger}_{2} \quad (6)$$

The sum $\Delta V^{\ddagger}_{-2} + \Delta V^{\ddagger}_{2}$ is equal to the partial molar volume change $\Delta \bar{V}_{-2}$ upon formation of contact pair intermediate [BHm CO] from the separated reactants (i.e., the pressure dependence of the "equilibrium constant" for formation of the contact pair intermediate). With the present data it is difficult to estimate the magnitude of this parameter separately. However, in the absence of bond formation between the two reactants, it is likely that the magnitude of $\Delta \bar{V}^{\ddagger}_{-2}$ will be small. If this were so, then the large negative $\Delta \bar{V}^{\ddagger}_{obs}$ apparently would largely reflect the pressure effect on the formation of the Fe–CO bond, i.e., $\Delta \bar{V}^{\ddagger}_{-1}$. This would also appear to be the result for the reaction in the mixed mineral oil/toluene solutions at low pressure.

For the case of diffusion limited rates, $k_{-1} \gg k_2$, and eq 5 becomes

$$\Delta V^{\ddagger}_{obs} = \Delta V^{\ddagger}_{-2} + \Delta V^{\ddagger}_{-1} + RT\left(\frac{d \ln k_{-1}}{dP}\right)_T = \Delta V^{\ddagger}_{-2} \quad (7)$$

and the pressure effect is dominated by changes in the second-order diffusion rate limit for the species and solvent under investigation owing to viscosity increases. The diffusion rate can be estimated by the relationship

$$k_d = \frac{8RT}{2000\eta} \quad (8)$$

where η is the viscosity.[35] Although the viscosity/pressure profile for the mixed toluene/mineral oil solvent is unknown, activation volumes as large as +20 cm^3 mol^{-1} have been noted for the viscous flow of toluene and of acyclic alkanes.[33] Neuman et al.[36] have shown that radical collapse rates can be increased by five- to sixfold with 3000 atm of pressure and diffusion rates can be reduced by at least this much with the increase in viscosity engendered by pressure increase. The product of these changes could easily exceed 40, and this would constitute a change from activation to diffusion control with a concomitant change from negative to positive activation volume. Pressure studies on diffusion limiting electron and energy transfer quenching of the metal complex and organic donor excited states have revealed positive $\Delta \bar{V}^{\ddagger}_{d}$ values in the range +7.5 to +9.5 for the organic solvents dichloromethane, tetrahydrofuran, ethanol and acetonitrile.[37] Thus a significantly positive value for $\Delta \bar{V}_{-2}$ would certainly be the expected result in the diffusion rate limit. One may conclude that the strongly positive $\Delta \bar{V}^{\ddagger}_{obs}$ values seen for experiments carried out in the mineral oil/toluene solutions in the high-pressure regime reflect the onset of diffusion limiting kinetics under these circumstances. What is remarkable is the very rapid crossover of this reaction from an activation dominated rate limit at low pressure to a diffusion limited rate at high pressure.

(32) The data in Figure 5 were curve fitted by a general least-squares refinement procedure available in the Kaleidagraph software package for the Macintosh. The starting point for this procedure was the expression for the observed first-order rate constant, $k_{obs} = k_{-1}k_{-2}[CO]/(k_{-1} + k_2)$. From here we had to establish the functional dependence of each term with respect to pressure. The bond formation rate constant, k_{-1}, as a function of pressure was found by integrating the expression for the volume of activation. This gave two parameters that were fitted, $\Delta V^{\ddagger}_{-1}$ and C_1, which is a constant of integration and also the exponential prefactor in the rate expression. The two diffusive rate constants, k_2 and k_{-2}, were found by equating the definition of the pressure coefficient of viscosity and the activation energy of viscosity (ref 33) and integrating. This gave an expression for viscosity as a function of pressure which was then inserted into the formula for a diffusion controlled rate constant. This gave $\Delta V^{\ddagger}_{-2}$, the activation volume for diffusion, and C_2, the exponential prefactor, the other two parameters that were fitted. The CO concentration was corrected by extrapolating and interpolating data for the compressibility of *n*-decane to 23 °C.[29] These numbers were normalized to a value of 1 at ambient pressure and curve fitted to a second degree polynomial ($R = 0.978$). The polynomial expression was divided into the ambient pressure [CO] to calculate [CO] at higher pressure. The $\Delta V^{\ddagger}_{-1}$ and $\Delta V^{\ddagger}_{-2}$ values which gave the curve fit illustrated in Figure 5 are −21 ± 10 and +16 ± 5 cm^3 mol^{-1}, respectively.

(33) Issacs, N. S. *Liquid Phase High Pressure Chemistry*; J. Wiley & Sons: New York, 1981; pp 102–108.

(34) Marsters, J. Ph.D. Dissertation, University of California, San Diego, 1989.

(35) Turro, N. J. *Modern Molecular Photochemistry*; The Benjamin/Cummings Publishing Co., Inc: Menlo Park, CA, 1978; p 314.

(36) (a) Neuman, R. C., Jr.; Bussey, R. J. *J. Am. Chem. Soc.* **1970**, *92*, 2440–2444. (b) Neuman, R. C., Jr. *Acc. Chem. Res.* **1972**, *5*, 381–387.

(37) (a) Crane, D. R.; Ford, P. C. *J. Am. Chem. Soc.* **1991**, *113*, 8510–8516. (b) Crane, D. R.; Ford, P. C. In preparation.

The quantum yields for carbon monoxide dissociation should also reflect the differing pressure dependencies of the respective rate constants. At ambient pressure in toluene and in the mineral oil/toluene solutions, the quantum yield for carbon monoxide dissociation has been estimated as unity.[34] The quantum yield of carbon monoxide dissociation to the fully separated species can be defined as

$$\phi_d = \phi_i\left(\frac{k_2}{k_2 + k_{-1}}\right) \quad (9)$$

where ϕ_i is the quantum yield for formation of the contact pair intermediate. If it is assumed that ϕ_i is unity and, furthermore, that ϕ_i is independent of pressure, then the changes in ϕ_d can be attributed to pressure-induced changes in the two rate constants k_2 and k_{-1}. At ambient pressure a quantum yield of unity clearly implies that $k_2 \gg k_{-1}$, consistent with the observation that formation of the BHmCO species from the photodissociated products is activation limited (case 1 above).

The quantum yields observed are in agreement with the three-state model (eq 1) and show that the quantum yield continuously decreases as pressure increases, consistent with the effects of pressure on the rate ratios in eq 3, i.e., that k_2 decreases while k_{-1} increases with increasing pressure.

Mechanisms of Thermal and Photochemical Processes. The objective of picosecond and nanosecond kinetic studies of heme–ligand systems is to understand the details of the thermal processes as they relate to biological oxygen transport. It is therefore important to establish that the photoprocesses actually relate to corresponding thermal processes. There are several ways to check this relationship by testing the predictions of thermal behavior from photochemical studies. For example, the dissociation rate should relate to quantum yield

$$k_{obs}^{CO} = k_1\frac{k_2}{k_2 + k_{-1}} \quad (10)$$

from which eq 9 becomes

$$k_{obs}^{CO} = k_1\phi_d/\phi_i \quad (11)$$

and the off rate (k_{obs}^{CO}) will correlate with the quantum yield as viscosity etc. is changed. We report this relationship elsewhere.[17d]

The present studies also serve to document a close relationship between the picosecond kinetics and derived values of k_{-1} and k_2 with ground-state kinetic behavior. The change of $\Delta V^{\ddagger}$ and Φ_{obs} with viscosity were predicted from picosecond kinetic studies and their discovery provides additional evidence that picosecond kinetic measurements reveal the rate constants for the thermal processes such as those in biological dioxygen transport. This point is made especially clear by the mathematical fitting of the data to the three-state system defined by picosecond measurements.

While we cannot assign the values of the rate constants of eq 1 for carbon monoxide binding at various pressures until picosecond measurements are made, the qualitative results are in agreement with values which were previously assigned based upon the assumptions that k_2 and k_{-2}, being diffusion constants, are similar for small molecules such as methyl isocyanide, dioxygen, and carbon monoxide. These values were confirmed by picosecond measurements of carbon monoxide binding to chelated protoheme in glycerol at 1 atm of pressure. Table I gives values of k_{-1}, k_2, and k_{-2} which have to be determined or estimated.

The high-pressure values for carbon monoxide are estimated on the basis of the usual effect of pressure on cage collapse processes and on diffusion rates. The positive $\Delta V^{\ddagger}$ at 3000 atm requires that $k_{-1} > k_2$.

Relevance to Heme Proteins. An important conclusion from Table I is that the behavior of carbon monoxide differs from those of other ligands. The fact that $k_2 \approx 30k_{-1}$ for carbon monoxide at normal pressure means that geminate recombination of carbon monoxide cannot be seen at low hydrostatic pressures or low viscosities. Therefore ligands such as isocyanides or nitric oxide would be better than carbon monoxide for studying the details of reactions in heme proteins. Oxygen displays two distinct

Table I. Rate Constants for Ligands Binding to the 1-Methylimidazole Complex of Protoheme Dimethyl Ester,[a] Chelated Protoheme, and Myoglobin

ligand	$10^{-10}k_{-1}$, s^{-1}	$10^{-10}k_2$, s^{-1}	$10^{-8}k_{-2}$, M^{-1} s^{-1}	ref
MeNC[a]	8, 11[c]	4	3	7
t-BuNC[a]	7	4	2.2	7
TMIC[a]	6.5	3.5	2.6	7
1-MeIm[a]	10	2	2.3	7
CO[a,b]	0.1	3	2.6	17
CO (3 katm)[b]	~0.4	<0.4	<3	this work
O_2[d]	1.4	1.5	0.046 (s^{-1})	6

[a] Solvent: toluene/1-MeIm, 80:20 by volume. [b] Protoheme–3-(1-imidazolyl)propylamide methyl ester chloride. Solvent: toluene. [c] Solvent: toluene. Data are taken from ref 17c. [d] Sperm whale myoglobin.

geminate processes in myoglobin as do isocyanides,[16] one in the picosecond range and the other in the subnanosecond range. Studies of isocyanides binding to myoglobin[6] provide the rate constants for reaction 12.[38]

$$\text{Mb–CN-}t\text{-Bu} \underset{k_1 = 6\times10^{10}\ s^{-1}}{\rightleftharpoons} \underset{\text{contact pair}}{[\text{Mb CN-}t\text{-Bu}]} \underset{k_{-2} = 5.2\times10^{6}\ s^{-1}}{\overset{k_2 = 4\times10^{10}\ s^{-1}}{\rightleftharpoons}} \underset{\text{separated pair}}{[\text{Mb//CN-}t\text{-Bu}]} \underset{k_{-3} = 4.2\times10^{3}\ M^{-1}\ s^{-1}}{\overset{k_3 = 3.6\times10^{6}\ s^{-1}}{\rightleftharpoons}} \text{Mb} + t\text{-BuNC} \quad (12)$$

With carbon monoxide, no picosecond relaxation was seen and we therefore cannot assign k_{-1} for myoglobin. Concentration-independent relaxations after photolysis of heme protein–CO complexes have been observed in several laboratories[19,22-25] with rate constants ranging from 10^6 to 10^9 s^{-1}. On the basis of the present results it seems possible that all of these processes except those with values near 10^9 s^{-1} are not bond-making processes but are the processes which assemble the contact pair, the k_2 and k_{-2} processes which have been called "matrix processes" or "protein separated pair" reactions. Thus in hemoglobin only one geminate relaxation is observed with $k_{obs} = 5 \times 10^6$ s^{-1}, rather similar to the second kinetic decay process observed with MbCNMe.[17] We suggest that there might also be carbon monoxide bond-forming reaction in hemoglobin or myoglobin with a rate constant of 10^9 s^{-1} but having a very low return yield. This is based, in part, on the observation that other ligands such as isocyanides, nitric oxide, and imidazole have values of k_{-1} which vary little between model compounds and heme proteins.[6,7,15] But no example of two concentration-independent relaxations (such as those reported for O_2, NO, and isocyanides) has been observed with CO as the photolyzed ligand. This matter deserves further investigation.

The inversion of $\Delta V^{\ddagger}$ should not occur for ligands such as isocyanides, imidazole, pyridines, ethers, nitric oxide, etc., because they all react with diffusion control, i.e., k_{-1} is in the range 10^{10} to 10^{11} s^{-1} for these ligands, but this phenomenon should not be confined to carbon monoxide. Any combination in which the bond-making step has a reduced rate constant, e.g., $k_{-1} \cong 10^9$ s^{-1}, will show a similar effect. There is a whole class of such reactions in which the proximal base is sterically hindered (T-state models); this class is exemplified in eq 13. When this hindered base was

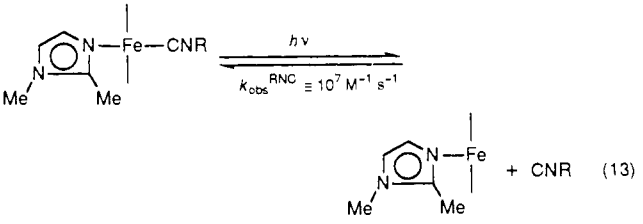

used, a reduced overall binding rate and an absence of picosecond

(38) Recent redeterminations of k_{-1} and k_2 for *t*-BuNC require these changes from the original values.[17]

return of MeNC or t-BuNC at low viscosities were observed. Such reactions should also show an inversion of $\Delta V^{\ddagger}$. These and other near diffusion controlled reactions are under study both to clarify their reaction mechanisms and to probe the generality of this pressure-viscosity method.

Acknowledgment. Studies at U.C. Santa Barbara were supported by grants to P.C.F. from the National Science Foundation (CHE 87-22561 and CHE 90-24845). Studies at U.C. San Diego were supported by grants from National Institutes of Health (PHS HL 13581).

Registry No. CO, 630-08-0; MCPH-CO, 140361-24-6; protoheme-3-(1-imidazolyl)propylamide methyl ester chloride, 72177-42-5.

Molecular and Electronic Structures of Pentaammineruthenium(II)-Thioether Complexes. The Nature of Ru(II)-S Back-Bonding Elucidated by Structural, Electronic Spectral, and Molecular Orbital Studies

Karsten Krogh-Jespersen,* Xiaohua Zhang, Yanbo Ding, John D. Westbrook, Joseph A. Potenza,* and Harvey J. Schugar*

Contribution from the Department of Chemistry, Rutgers, The State University of New Jersey, New Brunswick, New Jersey 08903. *Received November 4, 1991*

Abstract: The nature of Ru(II)-S(thioether) bonding has been probed by a combination of structural, spectroscopic, and computational methods. The synthesis, X-ray structure, and electronic spectra are presented for the $(NH_3)_5Ru[S(CH_3)(C_2H_5)]\cdot 2PF_6$ complex which crystallizes in the monoclinic space group $P2_1/n$ with $a = 8.3664$ (5) Å, $b = 12.337$ (1) Å, $c = 17.780$ (1) Å, $\beta = 100.388$ (5)°, $V = 1805.1$ (4) Å^3, $Z = 4$, and $R_F(R_{wF}) = 0.042$ (0.072) for 3475 reflections. The structure contains approximately octahedral $(NH_3)_5RuS(Me)Et^{2+}$ cations separated by disordered PF_6^- anions. The Ru(II)-N distances span the range 2.135 (4)-2.168 (4) Å and average 0.043 Å longer than those of the Ru(III) analogue. In contrast, the Ru(II)-S distance of 2.316 (1) Å is 0.055 Å shorter than that of the Ru(III) analogue, implying substantial back bonding. Structural parameters of the coordinated thioether in both Ru(II)- and Ru(III)-thioether complexes are close to those reported for the free ligand. Ab initio molecular orbital (MO) calculations have been performed on the ground state of the $(NH_3)_5Ru^{II}S(CH_3)_2$ complex with full geometry optimizations carried out at the Hartree-Fock (HF) level; partial geometry optimizations were made with correlation energy corrections included via Moller-Plesset perturbation theory (MP2, MP3). Good agreement between calculated and experimental structures is obtained only at the correlated (MP2, MP3) levels; at the HF level, the Ru(II)-S distance is computed more than 0.2 Å too long. Electronic population analyses at both the HF and MP2 levels are used to elucidate the metal-thioether interactions, in particular with respect to the nature of Ru(II)-S back bonding. Semiempirical MO calculations (INDO/S) using singly excited configuration interaction (SECI) and time-dependent Hartree-Fock (TDHF) methods permit assignment of the electronic spectra. Two Ru-thioether MLCT transitions are located in the 35 000-40 000-cm^{-1} region; in addition, a LMCT transition occurs at slightly higher energy (~45 000 cm^{-1}).

Introduction

Structural parameters and properties of the kinetically stable six-coordinate $(NH_3)_5Ru^{II}L$ and $(NH_3)_5Ru^{III}L$ complexes reflect electronic interactions of the ligand L with the metal d-orbitals. It is well-known that the electron rich t_{2g}^6 $(NH_3)_5Ru^{II}L$ complexes are preferentially stabilized if L is a π-acceptor and that the t_{2g}^5 $(NH_3)_5Ru^{III}L$ complexes, having a vacancy in the metal ion t_{2g} level, are stabilized when L is a π-donor. This ligand dependency of complex stability has been quantitated by extensive electrochemical studies of the Ru(II)/Ru(III) redox potentials in such systems.[1-3] The range of ligand π-acceptors to π-donors has been varied from N_2 to OH^-, and the resulting changes in redox potentials span 1.5 V.[3] Ligands may be ranked according to their affinities[3] for Ru(II) or Ru(III) and in an electrochemical series[4] according to their π-accepting/donating behavior.

Structural consequences of these π-bonding effects have been the subject of several crystallographic studies. When L is a π-acceptor such as pyrazine[5] or *N*-methylpyrazinium,[6] the Ru(II)-L bond distances are 0.07 or 0.13 Å shorter than the corresponding Ru(III)-L distances. In contrast, the Ru(II)-NH_3 bonds involving the purely σ-donating ammine ligands average about 0.03 Å longer than the Ru(III)-NH_3 bonds. Combined structural, spectroscopic, and computational studies of the $(NH_3)_5Ru^{III}L$ system in which L = imidazole (histidine) indicated that the strong σ-donor/weak π-donor nature of imidazole was responsible for the Ru(III)-imidazole bond being even shorter than the Ru(III)-N bonds to the above types of heterocyclic π-acceptor ligands.[7]

There has been considerable interest in the systems for which L = thioether. Thioether preferentially binds to and stabilizes the $(NH_3)_5Ru^{II}$ unit.[1] The resulting increase in the Ru(II) oxidation potential is comparable to that achieved by π-acceptor ligands such as pyridine, phosphine, or nitrile.[1,2,4] The kinetic stabilities of both the Ru(II)- and Ru(III)-thioether bonds allow the synthesis of mixed-valence systems with $(NH_3)_5Ru^{II,III}$ units linked by variable length oligospirocyclobutanes terminated by ligating thietanes.[8-12] These weakly coupled metal ion chro-

(1) Kuehn, C. G.; Taube, H. *J. Am. Chem. Soc.* **1976**, *98*, 689.
(2) Matsubara, T.; Ford, P. C. *Inorg. Chem.* **1976**, *15*, 1107.
(3) Lim, H. S.; Barclay, D. J.; Anson, F. C. *Inorg. Chem.* **1972**, *11*, 1460.
(4) Lever, A. B. P. *Inorg. Chem.* **1990**, *29*, 1271.
(5) Gress, M. E.; Creutz, C.; Quicksall, C. O. *Inorg. Chem.* **1981**, *20*, 1522.
(6) Wishart, J. F.; Bino, A.; Taube, H. *Inorg. Chem.* **1986**, *25*, 3318.
(7) Krogh-Jespersen, K.; Westbrook, J. D.; Potenza, J. A.; Schugar, H. J. *J. Am. Chem. Soc.* **1989**, *109*, 7025.
(8) Stein, C. A.; Taube, H. *J. Am. Chem. Soc.* **1981**, *103*, 693.
(9) Stein, C. A.; Lewis, N. A.; Seitz, G. *J. Am. Chem. Soc.* **1982**, *104*, 2596.
(10) Lewis, N. A.; Obeng, Y. S. *J. Am. Chem. Soc.* **1988**, *110*, 2306.
(11) Lewis, N. A.; Obeng, Y. S.; Taveras, D. V.; van Eldik, R. *J. Am. Chem. Soc.* **1989**, *111*, 924.

0002-7863/92/1514-4345$03.00/0